

Review

Application of inkjet printing to tissue engineering

Thomas Boland¹, Tao Xu¹, Brook Damon² and Xiaofeng Cui¹¹Department of Bioengineering, Clemson University, Clemson, SC, USA²Department of Physics and Astronomy, University of Missouri, Columbia, MO, USA

Recent advances in organ printing technology for applications relating to medical interventions and organ replacement are described. Organ printing refers to the placement of various cell types into a soft scaffold fabricated according to a computer-aided design template using a single device. Computer aided scaffold topology design has recently gained attention as a viable option to achieve function and mass transport requirements within tissue engineering scaffolds. An exciting advance pioneered in our laboratory is that of simultaneous printing of cells and biomaterials, which allows precise placement of cells and proteins within 3-D hydrogel structures. This advance raises the possibility of spatially controlling not only the scaffold structure, but also the type of tissue that can be grown within the scaffold and the thickness of the tissue as capillaries and vessels could be constructed within the scaffolds. Here we summarize recent advances in printing cells and materials using the same device.

Received 2 June 2006
Accepted 6 July 2006**Keywords:** Cell printing · Scaffold · Printing

1 Introduction

There are obvious and acute needs for human organs, such as heart, lungs, liver, kidney, pancreas for transplantation. The U.S. national patient waiting list for organ transplantation consists of more than 80 000 patients, of which 17 will die today (data from: Health Resources and Services Administration, U.S. Department of Health and Human Services). The shortage of donor organs prompted several approaches that were proposed to solve the problem: artificial mechanical organs, xenotransplantation (using animal organs), tissue engineering and regenerative medicine. While some artificial organs are already available to patients, they significantly reduce the quality of life and may have many unwanted site effects. Xenotransplantation, especially using organs from transgenic animals with reduced capacity to induce acute immune

response after transplantation and when combined with emerging methods of immunotolerance management are very promising. However, there is still great concern about potential spreading of animal viruses [1] and the long-term psychological effects of immunosuppressants that were revealed in the hand allograft studies [2].

Tissue engineering and regenerative medicine, which seek to repair injured or ill organs *in vivo* using cell transplantation, is a particularly promising approach to solving the need for replacement of failed organs. Furthermore, the need for engineered tissues and organs is not limited to the transplantation of failing vital organs; it has the potential of widespread use for *in vitro* applications, such as the use of perfused 3-D human tissue for toxicological research, drug testing and screening, or personalized medicine.

The classical tissue engineering approach is based on using pre-formed solid rigid scaffolds and isolated cells first proposed by Langer and Vacanti [3]. This approach combines expanding cells from the patient, seeding those cells on porous biodegradable scaffolds, culturing the constructs in a bioreactor, and implanting the resulting cell mass. While this approach has yielded in some unprecedented success for hollow organs [4], there are, however, at least three concerns with applying this approach to non-hollow organs:

Correspondence: Dr. Thomas Boland, Department of Bioengineering, Clemson University, Clemson, SC 29634, USA

E-mail: tboland@clemson.edu

Fax: +1-864-656-4466

Abbreviations: RP, rapid prototyping; SFF, solid free-form fabrication

1. Cell penetration and seeding is not very effective. Tissue maturation proceeds on the time scale of months and is not uniform throughout the scaffold. Although there is significant progress in designing scaffold allowing effective seeding and cell migration [5], the approach is still far from optimal.
2. Organs usually consist of many cell types and placing different cell types in specific positions represents a challenge that is still far from being resolved.
3. The pre-formed rigid scaffolds made from PLGA are not optimal for engineering contractile tissue such as heart, vascular tubes, or capillaries.

It is a generally accepted hypothesis that effective vascularization of tissue engineered constructs is a key to build larger tissues or organs [6]. A simple, yet very effective method for building blood vessels is that of rolling two-dimensional cell sheets into tubes [7]. While it cannot be adapted for complex three-dimensional organs, this approach, nevertheless, demonstrated that a direct placing mechanism has promise in creating three-dimensional vasculature. The scaffold and its porous architecture design play a significant role in tissue regeneration by preserving tissue volume, providing temporary mechanical function, and delivering growth factors and drugs. One approach to solve the vascularization issue is to engineer small diameter vessels and capillaries within the scaffold through a combined solid freeform fabrication and cell placement approach [8].

Several groups have designed and built scaffolds with controlled architecture. Complex hierarchical scaffold designs can only be built using layer-by-layer fabrication processes known collectively as solid free-form fabrication (SFF). A number of recent articles have reviewed and contrasted SFF scaffold fabrication techniques [9–11]. All SFF systems build a 3-D structure by layering a 2-D material onto a moving platform. Commercially available systems either photopolymerize liquid monomer, sinter powdered materials, process material either thermally or chemically as it passes through a nozzle, or print material, such as chemical binder onto powders. Recently, biomaterial scientists have used a number of these methods to fabricate tissue engineering scaffolds, including physical models of hard and soft tissues and custom-made tissue implant prostheses. Many of these rapid prototyping (RP) technologies can offer effective ways to precisely control matrix architecture (size, shape, interconnectivity, geometry and orientation) of a scaffold, yielding biomimetic structures of varying design and material composition. Hierarchical design of the scaffolds with micro-to millimeter features have demonstrated that enhanced control over mechanical properties, biological effects and degradation kinetics of the scaffolds is possible [12]. Moreover, SFF techniques can be easily automated and integrated with imaging techniques to produce constructs that are customized in size and shape allowing tis-

sue-engineering grafts to be tailored for specific applications or individuals [10].

As fabrication feasibility has been amply demonstrated, the critical issue has shifted to show the designer scaffolds outperform traditional scaffolds, because in spite of these advances, the current SFF techniques have yet to lead to harmonically organized complex tissue constructs. The primary hurdles to overcome are the same as in the classical tissue engineering approach: the building of capillaries and the exact placement of cell populations throughout the scaffold. Additionally, toxic solvents or high temperatures are still widely used in most SFF techniques, which are not suitable to many engineered tissue devices and limit their further applications in tissue engineering [13]. Thus, adapting existing SFF technologies to tissue engineering continues to be a genuine challenge.

2 Inkjet printing

Inkjet printing is a non-contact reprographic technique that takes digital data from a computer representing an image or character, and reproduces it onto a substrate using ink drops [14]. In addition to its well-known application in the word processing as an automation office tool, the inkjet technology has been widely employed in electronics and micro-engineering industries to print electronic materials [15]. Complex integrated circuits, such as polymer thin-film transistors have been generated by this low-cost fabrication method [16]. Recently, the inkjet technology has been successfully adapted to medicine and biomedical engineering applications, such as drug screening, genomics, and biosensors [17–19]. Although biological molecules and structures are often viewed as fragile, molecules such as DNA have been directed onto glass by commercial inkjet printers to fabricate high-density DNA micro-arrays without molecular degradation [20]. In addition, proteins such as horseradish peroxidase have been deposited onto cellulose paper to create active enzyme arrays for bioanalytical assays [21]. We have shown that active biosensors based on biotin-streptavidin linkages can be deposited onto glass [22].

More recently, a novel concept of inkjet printing cells and biomaterials by using the off-the-self printers to generate 3-D scaffolds and cellular structures has been proposed [23]. Commercially available desktop printers were modified to perform diverse tasks, such as printing self-assembled monolayers, proteins, and other molecules [24]. Based on the initial success in adapting printers to these tasks, the concept of organ printing was proposed [13]. Organ printing, defined as computer-aided jet based tissue engineering, is an advance in SFF as it allows constructing a 3-D object with living biological material, such as a specific cell type, tissue or organism. A fundamental requirement of this process is its capability of simultaneously delivery scaffolding materials, living cells, nutrients, therapeutic

drugs, growth factors, and or other important chemical components at the right time, right position, right amount and within the right environment to form living cells/extracellular matrix (or scaffold) for *in vitro* or *in vivo* growth. Here, we present an overview of our work demonstrating that a single device can perform these tasks.

3 Cell printing using thermal inkjet technology

While many of the top-down fabrication techniques used to build microelectromechanical systems, including photolithography, are attractive for organ printing due to the similar feature sizes, they are not suitable for delicate biological systems or aqueous environments. Our approach to 3-D organ printing technology is based on the delivery of controlled volumes of liquid to defined 3-D locations also known as drop-on-demand printing. Much progress in drop-on-demand printing has been made since the first patent by Siemens [25], which was based in Lord Kelvin's theory of jet break-up [26]. Thermal inkjet printing technology was invented by Hewlett-Packard and Canon Inc. in 1979, and has been improved continuously. For applications in our laboratory, we use inkjet pens with larger drop volumes such as the HP DeskJet pens, which have a drop volume of 80 pL. These pens have 50 firing chambers, where the actual heating occurs during 10- μ s pulse. The energy supplied to the ink during this process is dissipated into kinetic energy of the drop and heating of the drop. Modeling studies have indicated that the bulk drop temperature in the ink rises between 4 and 10 degrees above ambient during printing, which makes it possible to be used with living systems [27]. We have successfully used inkjet printers to print cell suspensions. The modifications to the printers have been previously described in detail [22]. In brief, the paper feed sensor mechanism of the printers was disabled, the printer was placed inside a sterile hood, and sterilized by UV radiation. A sterile hydrogel sample was placed under the print head onto the ledge of the printer; in other experiments, sterile pre-wet-

ted porous nylon membranes that were placed onto hydrogels served as "paper". The print cartridges were thoroughly rinsed many times and cleaned with 70% ethanol solution. This cleaning protocol proved sufficiently sterile in all our experiments. Sterility was assessed by the absence of bacterial colonies on agar plates onto which autoclaved water was printed after incubating 5 days in a humid incubator at 36°C [27]. Two different cell types were used for the inkjet printing experiments. The first included primary neurons obtained from cortical regions of 10-day-old chicken embryos. The second type used was a quail mesoderm QCE-6 cell line, which is a multipotential mesodermal stem cell line. The QCE-6 cell line had been transfected to express green fluorescent protein. The modified HP Deskjet printer (HP 550C) and a cleaned HP 51626a ink cartridge were used to print the cells directly into specific patterns onto 1.5 mg/mL collagen hydrogels. After printing, the printed cells were placed into dishes and moved to an incubator, which was maintained at 37°C, 5% CO₂, and 99% relative humidity. The medium was changed every 1–2 days and the growth of the cells was monitored daily by light and epi-fluorescence microscopy. The culture medium for the primary neurons was Neurobasal (Gibco-BRL) supplemented with 2% B27, 0.5 mm L-glutamine and 25 mm 2-mercaptoethanol. The growth medium for QCE-6 cells was MEM with Earle's salt, nonessential amino acid, and L-glutamine, prepared as described previously [28].

QCE-6 cells were found to be dispersed on the collagen gel surface and to emit green fluorescence under epifluorescence microscopy, which may indicate viable cells. Furthermore, at the early stage of the culture, fewer cells were observed individually. After 6 days of culture, the number of cell increased and some clustering was observed, while after a 12 day culture most cells were clustered (Fig. 1). These observations suggest the QCE-6 stem cells still could maintain their viability and proliferate on the collagen gel after being printed. The ability to print cells at varying density is evident from the gradient shown in Fig. 1A and may be important in differentiation studies.

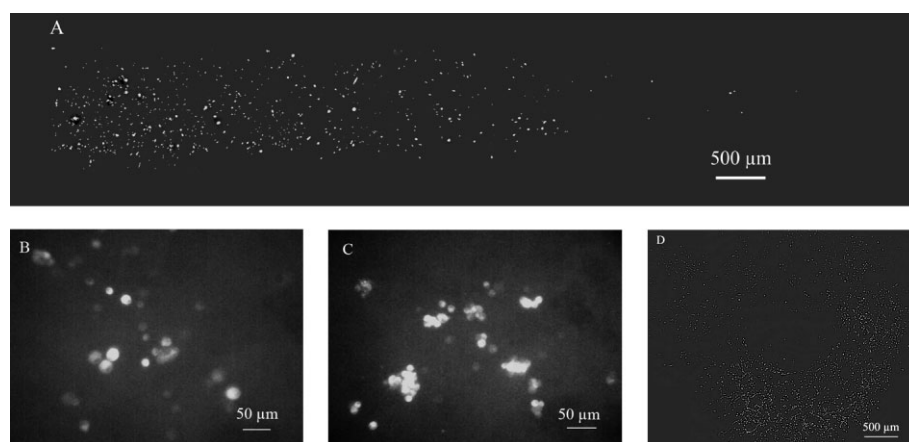


Figure 1. QCE-6 stem cells observed under a fluorescence microscope after being printed through the nozzles. (A) Gradient of cells on day 3. (B) Several individual cells on day 3 were found as individual cells. (C) At day 12 cells observed to be clustered are aggregated. (D) Ring of QCE-6 cells printed onto collagen gel on day 5.

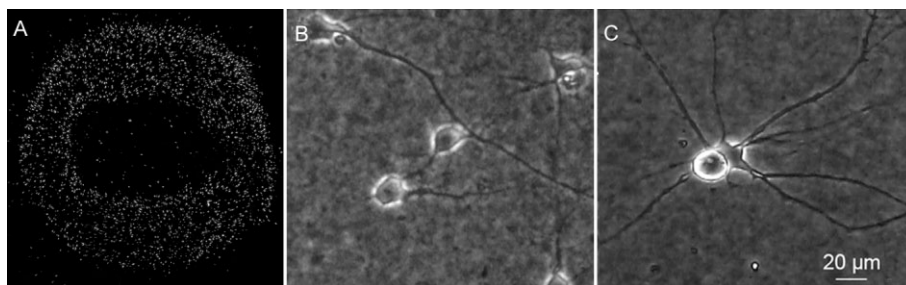


Figure 2. Primary cortical neurons were delivered by inkjet printing in the pre-designed ring patterns as indicated at day 1 utilizing bright field microscopy (A). At day 3 many of the neurons exhibited a characteristic neuronal morphology as seen with bright field microscopy (B). At day 7 the processes of two neurons have grown to about 40 μm in length (C). Magnifications: 40 \times (A), 100 \times (B, C).

A printed neuronal ring was obvious after 1 day in culture, as shown in Fig. 2A. Many rounded cells were seen, indicative of non-differentiated or dead cells. Few differentiated neurons with processes were obvious in the pattern at day 2 in culture, but after 5 days, many neurons began to differentiate and developed processes, exhibiting a polarized morphology (Fig. 2B, C). The survival of neurons was indicated by the outgrowth of their processes and the establishment of polarized morphologies. However, the lengths of the processes were shorter than that observed in the standard 2-D culture [29]. One of the possible reasons could be related to the use of a 3-D collagen gel. Prior studies have found that increasing collagen concentration will decrease the neurite outgrowth [30].

To assess whether the printed neurons still retained their neuronal phenotypes, immunostaining for MAP2 and neurofilament was carried out. The printed samples were fixed with 4% formaldehyde. After incubating in the blocking solution (2% BSA and 3% goat serum prepared in 1 \times PBS) overnight at 4–8 $^{\circ}\text{C}$, the samples were exposed to the primary antibody of mouse anti-MAP2 mAb and rabbit anti-neurofilament NF 150 mAb (Chemicon, Temecula, CA, USA) (1:150 dilution in PBS overnight at 4–8 $^{\circ}\text{C}$). Subsequently, fluorescence-labeled secondary antibodies were applied. The stained samples were photographed using the LSM-5 confocal microscope (Zeiss, Germany).

MAP2 and neurofilament are well-established neuronal markers for the identification of neuronal cell bodies, dendrites and neuronal axons. Whole-cell patch clamp recordings were also performed in a recording chamber placed on the stage of a Zeiss Axioscope upright microscope. Immunocytochemistry and patch clamp data are shown in Fig. 3. These data suggest that the rat embryonic cortical neurons maintained their neuronal phenotypes and ability to fire action potentials after being printed through the nozzles. ANOVA statistical analysis showed that none of the 16 parameters measured using the Axioscope, changed significantly when compared to manually plated controls ($n=16$, $p>0.05$) [31].

By replacing the regular print ink with the cell suspensions, this can be considered “bio-ink” that could be delivered using a commercial, thermal-based inkjet printer. Here we investigated whether fragile mammalian cells, the cells needed for building engineered tissues and organs, could be used as a bio-ink and printed directly by a commercial inkjet printer. Since the physiological properties of mammalian cells strongly depend on the culture conditions and they are much more sensitive to heat and mechanical stress, there was a major concern that the cells could be damaged or lysed by the conditions present during thermal printing. The present study indicates, however, that many viable cell types can be delivered us-

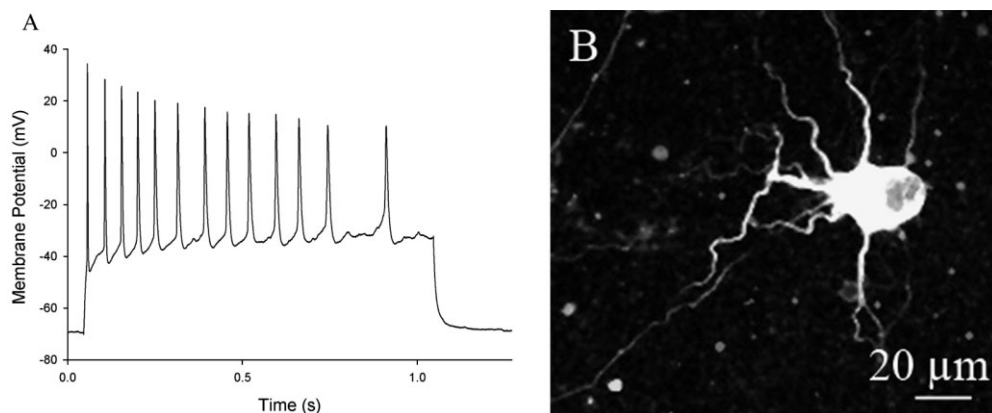


Figure 3. (A) Electrophysiological characterization of printed embryonic cortical neurons. Maximum action potential firing rate of a day 15 cortical neuron is shown. (B) Confocal microscopy image of printed neurons double stained with a neuronal marker after 15 days of culture. The cell bodies and dendrites of rat embryonic hippocampal neurons were immunoreacted with anti-MAP2 mAb (green), while the axons of the neurons were immunoreacted with anti-neurofilament mAb (red). Original magnification, 400 \times .

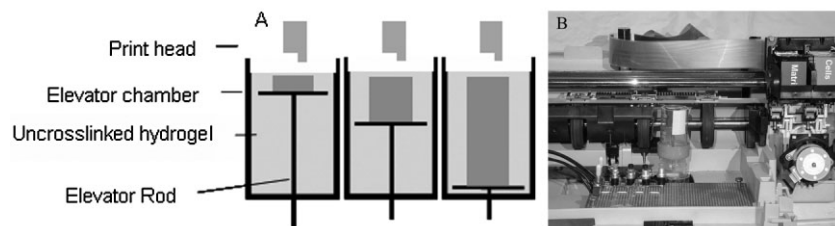


Figure 4. Schematic view and photograph of the moving platform inside the chamber. (A) After each printed layer, the elevator rod is lowered. Since the total volume inside the chamber is constant during the lowering of the stage, uncross-linked hydrogel will flood onto the printed areas. After the rod has reached the bottom of the chamber, a printed hydrogel structure is found on the stage. (B) Photograph of the chamber under a modified HP DeskJet. The chamber is removable and can be installed under many different printers.

ing a modified inkjet printer. These data confirm our previous analysis, that cells can survive thermal printing [27].

4 3-D printing of biomaterials using thermal inkjet printers

To build a 3-D structure, z-axis control through a moving platform was implemented using an electronically controlled chamber with an elevator stage. The elevator stage, a 2.5-cm round glass cover-slip is fixed to the tip of a metallic rod, controlled by a stepper motor, which itself is powered by a 4 V signal and operated through a series of four toggle switches. A customized sterile 50-mL conical tube is used as the chamber housing the elevator stage (Fig. 4). The elevator rod is sealed to the chamber with sterile silicone grease.

The chamber was filled with a 2% alginate solution, a liquid that is known to cross-link under mild conditions to form a biodegradable hydrogel scaffold [32]. The ink cartridge was filled with 0.25 M CaCl_2 , which is known to promote the cross-linking of the individual alginate chains resulting in a 3-D structure. This cross-linker was printed layer-by-layer, deep to superficial onto the platform resulting in 3-D structures by causing the gelling of the alginate solution at the air/solution interface. After cross-linking occurred, the platform was submerged into fresh un-cross-linked solution thus maintaining hydration of the gelled constructs while at the same time providing a new interface for the next layer. This re-coating procedure also insured that each layer bonded to the previous one. The procedure was repeated until the desired shape was obtained. Due to the relative small differences in density of the gelled constructs and the surrounding liquid, large structures can be fabricated with little deformation or collapse. The alginate acid can also be dissolved in low calcium cell medium, thus fabrication of scaffold under mild and cell friendly conditions is possible with this setup. A number of acellular structures were printed with this method, including tubes, branched tubes, and hollow cones (Fig. 5).

5 Microstructure and mechanical properties of printed hydrogels

How this fabrication of alginate hydrogels affects the structure and function of these hydrogels was investigated by SEM. These microscopy images reveal that each printed drop was hollow and contained no hydrogel material, while the area between drops showed solidified material. This can be explained by a surface gelling mechanism, in which the surface of the drop is gelled immediately after penetrating the solution, forming a capsule or shell. This shell will prevent the larger alginate molecules from penetrating, but will allow the smaller calcium ions to diffuse to the outside. The alginate acid in the periphery of the drop is then cross-linked, resulting in a second shell. As this shell formation and ion diffusion continues, layered structures of shells are formed. These are clearly visible in the cross-sectional SEM images of the shown in Fig. 6C.

The mechanical tensile properties of the pure and printed alginate hydrogels were measured. 3-D printed sheets were constructed as described above. To prepare manual samples, the 0.25 M CaCl_2 solution was directly poured into the 2% alginate solution and stored in a 6-well plate. Before complete gelling, forceps were used to take the partially gelled alginate out from the well and pull the

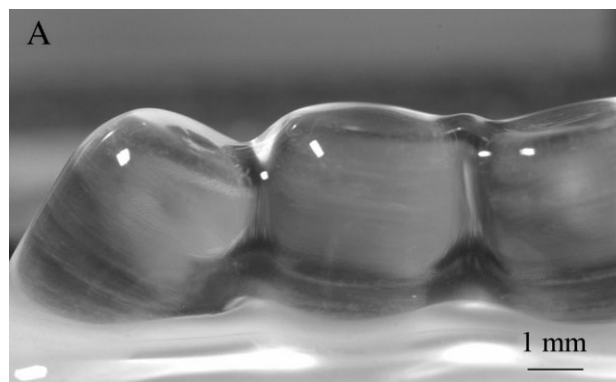


Figure 5. Photographs of printed tubes. (A) Parallel tubes are shown immediately after printing with the stage raised above the liquid level. (B) A branched chambered structure.

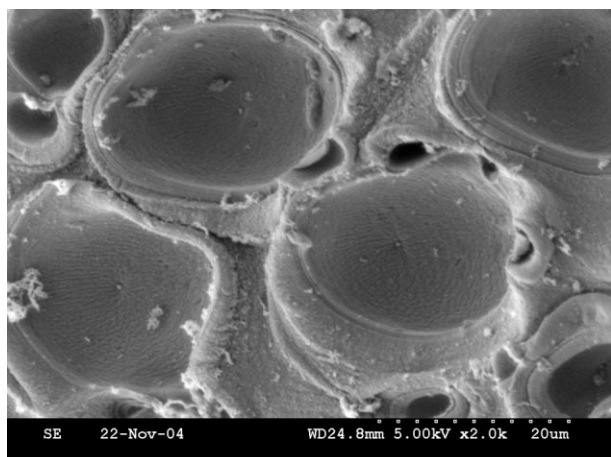


Figure 6. Microscopic views of printed alginate biomaterials SEM micrograph of a cross-sectional view of a printed sheet.

alginate gel into a long cylindrical tube with even diameter. The long tubes were cut into several segments for mechanical testing and kept in 0.25 M CaCl₂ solution overnight for complete cross-linking. The tensile properties of the different samples were then determined at room temperature by stretching the sample at a constant deformation rate of 5 mm/min. The un-axial tensile testing was performed using the MTS electromechanical

Table 1. Mechanical properties of manual and printed alginate hydrogels

	Young's Modulus (kPa)	UTS (kPa)
Manual	350 ± 80 (n=5)	220 ± 40 (n=5)
Printed	89 ± 47 (n=5)	56 ± 12 (n=5)

testing system (MTS Systems Corporation, Eden Prairie, MN, USA) and original data were acquired and analyzed by the software of TestWorks® (MTS System Corporation). The resulting stress-strain data were used to calculate the Young's modulus and ultimate tensile stress (UTS). The Young's modulus was defined as the slope of the linear portion of the stress-strain curve, which occurred in the range of 0–100% of the UTS. The peak stress achieved during mechanical testing was taken as the UTS. It can easily be seen from the data in Table 1, the printed samples have much lower properties due to the high porosity.

The diffusion of the cross-linker is concentration dependent; thus, by changing the concentrations of hydrogel and cross-linkers, a variety of structures can be obtained, ranging from amorphous to dots to channels. We undertook a detailed study on how different concentrations of alginate and cross-linker affect the fabricated hydrogels. These studies are summarized in Table 2. While cross-linker concentrations below 0.2 mmol/mL usually lead to amorphous materials, low alginate concentrations

Table 2. Microscopic views of printed alginate biomaterials. Color images are phase light micrographs, top view, 40x; black/white image is SEM micrograph of a cross-sectional view of a printed sheet. To fabricate alginate channels, best results are obtained with 8% alginate solution and 0.4 mmol/mL CaCl₂ (scale bar = 50 μm)

CaCl ₂ (mmol/ml)	Alginate (%)							
	0.5	2.0	3.0	5.0	6.0	8.0	10	12
0.1	X	X	X	X	X	X	X	X
0.2	X	X	X	X	X	X	X	X
0.3	X							
0.4	X							
0.5	X							

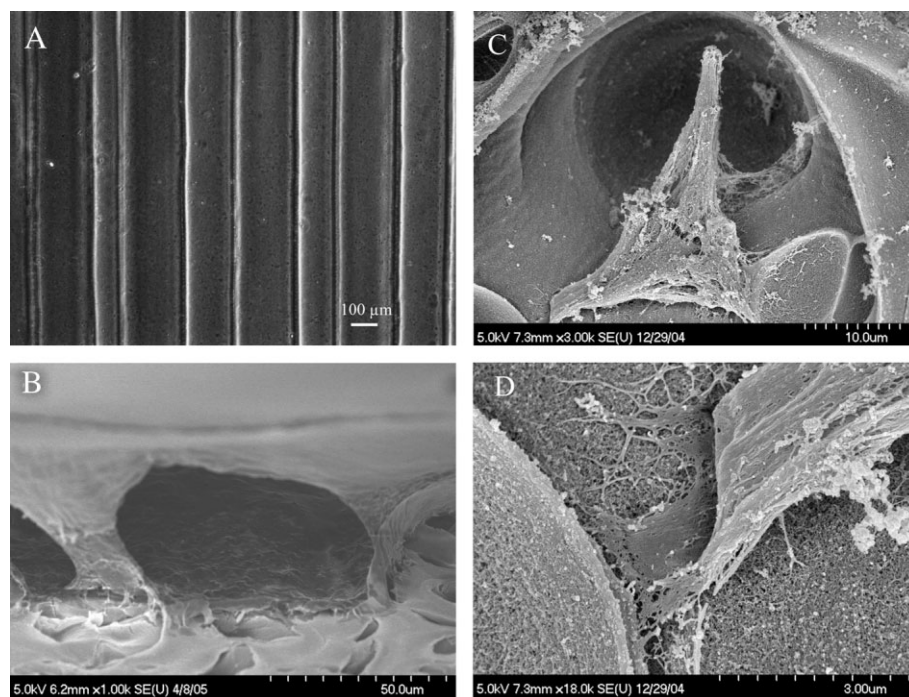


Figure 7. SEM and optical micrographs of printed alginate channels. (A) Top view of parallel channels of 30- μm diameter. Although some inhomogeneous sites are seen, the patterns transfer in general with better than 50- μm fidelity. (B) Cross-section through three alginate channels. (C) SEM image of an attached bovine aortal endothelial cell inside an alginate channel. The spread out form of the cell body indicates the attachment or motility of the cell. (D) Expanded area of the endothelial cell shown in (C). A portion of the cell cortex is seen with filopodia (f) and lamellapodia (l) protruding from the cell. The amorphous alginate material (a) can be seen covered with a fibrous material (c) near the lamellapodia at the trailing edge of the cell. As filopodia are typically involved in cell motility at the leading edge of cells, we conclude that this cell is moving along the channel, while depositing matrix material.

lead to structures with hollow shells and higher alginate concentrations lead to horizontal channels.

6 Simultaneous printing of materials and cells

Following those initial studies, the simultaneous printing of endothelial cells and cross-linker was investigated. Figure 7 shows channels fabricated by printing a line pattern of cross-linker at the 0.4 mmol/mL concentration (from Table 2) resulting in microchannel architectures. We examined endothelial cell attachment to these designer hydrogels by SEM. Filopodia can be seen at the leading edge of the cell and lamellapodia at the trailing edge, suggesting cell migration into the channels since these are typically involved in cell motility. Also, possible deposition of extracellular matrix is evident from the micrographs. This proves that the cells are able to attach and migrate in these gels after being exposed to the cross-linker, and that alginate may serve as a tissue engineering matrix.

7 Conclusions

Taken together, these preliminary data suggest that many cell types can be printed as bio-ink using inkjet printers; the cells survive, maintain their phenotype, differentiate and show function. Cells can be printed uniformly and homogeneously into confluent layers. Using a fast gelling hydrogel system, many layers of cells and hydrogels can be

printed into 3-D structures. Pores and channels of uniform size can be printed into the materials according programable patterns, and endothelial cells are seen to attach to the inside of printed hydrogel pores when printed simultaneously. Based on its unique characteristics of high-throughput efficiency, its cost effectiveness, and full automation, cell or organ printing is being examined for its potential to engineer new tissues or organs. However, there are considerable technical barriers in the development of this emerging inkjet printing technology, such as the ability of the modified printers to deliver viable cells and the capability of the inkjet printing to fabricate functional, viable and functionally vascularized 3-D constructs.

Vital to the cell patterning procedures is the use of stable, aqueous non-cytotoxic bioinks that act as cross-linking agents, and are delivered using the inkjet method. There is a need to develop biomaterials that can be used as bioinks; current strategies for bioinks include natural and synthetic physical hydrogels [33], concentrated cell pellets [13] and collagen solutions [24]. Clearly, this technology is still in its infancy and improvements in the biomaterials used as bioinks and scaffolds will be needed before any clinical applications can be realized. Optimizing the rheological and surface properties of the inks, and designing printers optimized for these properties will improve the cell density of the printed constructs, and the speed at which tissues may be manufactured. Incorporating controlled release particles loaded with growth factors or signaling molecules into bioinks opens interesting

avenues for combining cell printing with other potential therapeutic modalities. Thus we are just beginning to realize some of the potential of this technology.

The authors would like to thank C. Eisenberg for the QCE-6 cells. Brook Damon was supported by the NIH/NSF Bioengineering and Bioinformatics Summer Institute, grant number NSF ERB 0234082.

8 References

- [1] Mueller, N. J., Barth, R. N., Yamamoto, S., Kitamura, H. *et al.*, Activation of cytomegalovirus in pig-to-primate organ xenotransplantation. *J. Virol.* 2002, **76**, 4734–4740.
- [2] Kanitakis, J., Petruzzo, P., Jullien, D., Badet, L. *et al.*, Pathological score for the evaluation of allograft rejection in human hand (composite tissue) allotransplantation. *Eur. J. Dermatol.* 2005, **15**, 235–238.
- [3] Langer, R., Vacanti, J. P., Tissue engineering. *Science* 1993, **260**, 920–926.
- [4] Atala, A., Bauer, S. B., Soker, S., Yoo, J. J., Retik, A. B., Tissue-engineered autologous bladders for patients needing cystoplasty. *Lancet* 2006, **367**, 1241–1246.
- [5] Ma, P. X., Choi, J. W., Biodegradable polymer scaffolds with well-defined interconnected spherical pore network. *Tissue Eng.* 2001, **7**, 23–33.
- [6] Nerem, R. M., Seliktar, D., Vascular tissue engineering. *Annu. Rev. Biomed. Eng.* 2001, **3**, 225–243.
- [7] L'Heureux, N., Paquet, S., Labbe, R., Germain, L., Auger, F. A., A completely biological tissue-engineered human blood vessel. *FASEB J.* 1998, **12**, 47–56.
- [8] Alper, J., Bioengineering. Biology and the inkjets. *Science* 2004, **305**, 1895.
- [9] Hollister, S. J., Porous scaffold design for tissue engineering. *Nat. Mater.* 2005, **4**, 518–524.
- [10] Hutmacher, D. W., Sittinger, M., Risbud, M. V., Scaffold-based tissue engineering: rationale for computer-aided design and solid free-form fabrication systems. *Trends Biotechnol.* 2004, **22**, 354–362.
- [11] Tsang, V. L., Bhatia, S. N., Three-dimensional tissue fabrication. *Adv. Drug Deliv. Rev.* 2004, **56**, 1635–1647.
- [12] Leong, K. F., Cheah, C. M., Chua, C. K., Solid freeform fabrication of three-dimensional scaffolds for engineering replacement tissues and organs. *Biomaterials* 2003, **24**, 2363–2378.
- [13] Mironov, V., Boland, T., Trusk, T., Forgacs, G., Markwald, R. R., Organ printing: computer-aided jet-based 3D tissue engineering. *Trends Biotechnol.* 2003, **21**, 157–161.
- [14] Mohebi, M. M., Evans, J. R., A drop-on-demand ink-jet printer for combinatorial libraries and functionally graded ceramics. *J. Comb. Chem.* 2002, **4**, 267–274.
- [15] Sirringhaus, H., Kawase, T., Friend, R. H., Shimoda, T. *et al.*, High-resolution inkjet printing of all-polymer transistor circuits. *Science* 2000, **290**, 2123–2126.
- [16] Wang, J. Z., Zheng, Z. H., Li, H. W., Huck, W. T., Sirringhaus, H., Dewetting of conducting polymer inkjet droplets on patterned surfaces. *Nat. Mater.* 2004, **3**, 171–176.
- [17] Hughes, T. R., Mao, M., Jones, A. R., Burchard, J. *et al.*, Expression profiling using microarrays fabricated by an ink-jet oligonucleotide synthesizer. *Nat. Biotechnol.* 2001, **19**, 342–347.
- [18] Collier, W. A., Janssen, D., Hart, A. L., Measurement of soluble L-lactate in dairy products using screen-printed sensors in batch mode. *Biosens. Bioelectron.* 1996, **11**, 1041–1049.
- [19] Lemmo, A. V., Rose, D. J., Tisone, T. C., Inkjet dispensing technology: applications in drug discovery. *Curr. Opin. Biotechnol.* 1998, **9**, 615–617.
- [20] Okamoto, T., Suzuki, T., Yamamoto, N., Microarray fabrication with covalent attachment of DNA using bubble jet technology. *Nat. Biotechnol.* 2000, **18**, 438–441.
- [21] Roda, A., Guardigli, M., Russo, C., Pasini, P., Baraldini, M., Protein microdeposition using a conventional ink-jet printer. *Biotechniques* 2000, **28**, 492–496.
- [22] Pardo, L., Boland, T., A quantitative approach to studying structures and orientation at self-assembled monolayer/fluid interfaces. *J. Colloid Interface Sci.* 2003, **257**, 116–120.
- [23] Wilson, W. C. Jr., Boland, T., Cell and organ printing 1: protein and cell printers. *Anat. Rec. A Discov. Mol. Cell Evol. Biol.* 2003, **272**, 491–496.
- [24] Roth, E. A., Xu, T., Das, M., Gregory, C. *et al.*, Inkjet printing for high-throughput cell patterning. *Biomaterials* 2004, **25**, 3707–3715.
- [25] Elmqvist, R., *Measuring instrument of the recording type*, US Patent 2566443, 1951.
- [26] Rayleigh, J. W. S., On the instability of jets. *Proc. London Math. Soc.* 1878, **10**, 4–13.
- [27] Xu, T., Jin, J., Gregory, C., Hickman, J. J., Boland, T., Inkjet printing of viable mammalian cells. *Biomaterials* 2005, **26**, 93–99.
- [28] Eisenberg, C. A., Markwald, R. R., Mixed cultures of avian blastoderm cells and the quail mesoderm cell line QCE-6 provide evidence for the pluripotentiality of early mesoderm. *Dev. Biol.* 1997, **191**, 167–181.
- [29] Das, M., Molnar, P., Devaraj, H., Poeta, M., Hickman, J. J., Electrophysiological and morphological characterization of rat embryonic motoneurons in a defined system. *Biotechnol. Prog.* 2003, **19**, 1756–1761.
- [30] Baldwin, S. P., Krewson, C. E., Saltzman, W. M., PC12 cell aggregation and neurite growth in gels of collagen, laminin and fibronectin. *Int. J. Dev. Neurosci.* 1996, **14**, 351–364.
- [31] Xu, T., Gregory, C. A., Molnar, P., Cui X., *et al.*, Viability and electrophysiology of neural cell structures generated by the inkjet printing method. *Biomaterials* 2006, **27**, 3580–3588.
- [32] Atala, A., Cima, L. G., Kim, W., Paige, K. T. *et al.*, Injectable alginate seeded with chondrocytes as a potential treatment for vesicoureteral reflux. *J. Urol.* 1993, **150**, 745–747.
- [33] Boland, T., Mironov, V., Gutowska, A., Roth, E. A., Markwald, R. R., Cell and organ printing 2: fusion of cell aggregates in three-dimensional gels. *Anat. Rec. A Discov. Mol. Cell Evol. Biol.* 2003, **272**, 497–502.



Dr. Thomas Boland is Associate Professor of Bioengineering and directing the Nanoscale Biointerfaces Lab at Clemson University (South Carolina, USA). He studied engineering at the E.N.S.I.G.C. in Toulouse (France, 1990) and obtained his PhD in Chemical Engineering in 1995 at the University of Washington (DC, USA). At Penn State University he performed postdoctoral

research in the area of Materials Science, in 1997. Dr. Boland's current research interests cover atomic force microscopy, protein and cell printing, organ printing and biointerfaces.